

System-Level Performance Analysis of LoRa-Based LEO Satellite Constellations for IoT Communications

Quantao Yu, Deepak Mishra, *Senior Member, IEEE*, Hua Wang, *Member, IEEE*,
Dongxuan He, *Member, IEEE*, Jinhong Yuan, *Fellow, IEEE*, and Michail Matthaiou, *Fellow, IEEE*

Abstract—In this letter, we propose a novel spherical stochastic geometry (SG)-based analytical framework to characterize the system-level performance of Long-Range (LoRa)-based low Earth orbit (LEO) satellite constellations. Specifically, tractable analytical expressions for the uplink coverage probability and area spectral efficiency are derived, where the LEO satellite constellations and the terrestrial LoRa end-devices (EDs) are modeled by a binomial point process (BPP) and Poisson point process (PPP), respectively. Numerical simulations not only verify our theoretical analysis but also provide some useful insights into the practical implementation of LoRa-based LEO satellite constellations for Internet of Things (IoT) communications.

Index Terms—Internet of Things (IoT), Long-Range (LoRa), low Earth orbit (LEO) satellite constellations, performance analysis, stochastic geometry (SG).

I. INTRODUCTION

OVER the past few years, Long-Range (LoRa) has attracted widespread attention from both academia and industry due to its superior capabilities to provide energy-efficient and cost-effective communications for various Internet of Things (IoT) applications [1]. Moreover, with the emerging innovation of launch and propulsion technologies, as well as the rapid development of miniaturized satellites known as CubeSats [2], exploiting low Earth orbit (LEO) satellite constellations has become an efficient means to provide ubiquitous IoT connectivity especially in rural and remote areas [3]. In this context, an accurate system-level performance analysis of LoRa-based LEO satellite constellations is of great importance for the practical design and implementation of such a new paradigm.

To address this issue, the authors in [4] presented a single satellite network model to analyze the access probability of LoRa-based LEO satellite IoT systems. In [5], the authors investigated the uplink performance of IoT-over-satellite networks in terms of coverage probability and normalized throughput based on LEO satellite constellations. Moreover, the authors in [6] proposed a stochastic geometry (SG)-based

analytical framework for characterizing the coverage performance of IoT-over-satellite networks in both direct access and indirect access scenarios, where the IoT end-devices (EDs) and LEO satellite constellations were modeled by a Poisson cluster process (PCP) and binomial point process (BPP), respectively. However, the system models proposed in [5], [6] did not take into account the unique features of LoRa networks, including the chirp spread spectrum (CSS) modulation used in physical (PHY) layer and the duty cycle-limited random access employed in medium access control (MAC) layer, which however play a dominant role in determining the overall performance of LoRa-based LEO satellite constellations. To the best of our knowledge, an accurate system-level performance analysis of such a new paradigm has not been well investigated in the existing works.

In this letter, we focus on the system-level performance analysis of LoRa-based LEO satellite constellations to fill this gap, where the main contributions are summarized as follows:

- 1) A novel analytical framework for characterizing the system-level performance of LoRa-based LEO satellite constellations is proposed based on spherical SG, where both the channel characteristics of satellite communications and the unique features of LoRa networks are considered in our proposed system model.
- 2) Tractable analytical expressions for the uplink coverage probability and area spectral efficiency are derived under the BPP constellation model and Poisson point process (PPP) EDs model, where the trends of both performance metrics are unveiled with respect to some key system parameters, such as the density of LoRa EDs and the spreading factor (SF). In particular, the uplink coverage probability is demonstrated to be a monotonically decreasing function with respect to the EDs' density, while the area spectral efficiency is proven to be a unimodal function of the EDs' density.
- 3) Numerical simulations are conducted to corroborate our theoretical performance analysis and provide some useful insights into the practical design and implementation of LoRa-based LEO satellite constellations.

Notations: Throughout this paper, we denote $F_X(x)$ and $f_X(x)$ as the cumulative distribution function (CDF) and the probability density function (PDF) of a random variable X ; $\max\{\cdot\}$, $\lceil\cdot\rceil$, $\exp(\cdot)$, and $\ln(\cdot)$ are the maximum, ceiling, natural exponential, and natural logarithm operations; $\mathbb{E}[\cdot]$ and

Quantao Yu, Hua Wang, and Dongxuan He are with the School of Information and Electronics, Beijing Institute of Technology, Beijing 100081, China (e-mails: 3120215432@bit.edu.cn; wanghua@bit.edu.cn; dongxuan_he@bit.edu.cn).

Deepak Mishra and Jinhong Yuan are with the School of Electrical Engineering and Telecommunications, University of New South Wales Sydney, NSW 2052, Australia (e-mails: d.mishra@unsw.edu.au; j.yuan@unsw.edu.au).

Michail Matthaiou is with the Centre for Wireless Innovation (CWI), Queen's University Belfast, BT3 9DT Belfast, U.K. (e-mail: m.matthaiou@qub.ac.uk).

$\Pr\{\cdot\}$ denote the mathematical expectation and probability measure, respectively.

II. SYSTEM MODEL

In this section, we present our proposed analytical framework for LoRa-based LEO satellite constellations, including the network model, channel model, and signal model.

A. Network Model

1) *Constellation model*: Let us denote R as the radius of Earth. For the constellation model, we assume that there are N_s LEO satellites randomly distributed at the same orbit altitude H , while the satellite locations are characterized by a homogeneous spherically wrapped BPP Φ_s .

2) *EDs model*: The LoRa EDs are assumed to be uniformly distributed within the satellite footprint, whereas the distribution of the LoRa EDs is modeled by a PPP Φ with intensity λ (i.e., the density of LoRa EDs). Moreover, we consider that there are \mathcal{K} classes of LoRa EDs and each class of LoRa EDs is modeled by an independent PPP Φ_k with intensity λ_k , where $k \in \{7, \dots, 12\}$ denotes the SF value. For simplicity, random SF allocation scheme is considered in this paper, where each ED is randomly assigned a SF and the proportion that an ED is assigned the SF k is $\rho_k = \frac{1}{\mathcal{K}}, \forall k$. Therefore, the density of EDs of class k is given by $\lambda_k = \rho_k \lambda$.

All classes of LoRa EDs are equipped with an omnidirectional antenna with the same effective isotropic radiated power (EIRP) P_t . In addition, we denote Φ_k^A as the PPP of active LoRa EDs of class k with intensity $p_k \lambda_k$, where $p_k = \frac{T_k}{T_p}$ is the active probability with T_k and T_p representing the Time on Air (ToA) of class k and the average packet inter-arrival time, respectively. Specifically, the ToA of class k is given by [7]

$$T_k = \frac{2^k}{B} \left(N_p + 12.25 + \max \left\{ \left\lceil \frac{8L - 4k + 28 + 16C - 20E}{4k} \right\rceil (C_r + 4), 0 \right\} \right), \quad (1)$$

where B is the configured bandwidth, N_p is the number of preamble symbols, L denotes the PHY payload length in bytes, C_r is the code rate, C is the cyclic redundancy check (CRC) indicator, and E is the PHY layer header indicator.

3) *Geometric model*: As depicted in Fig. 1, we assume that each LoRa ED associates with its nearest satellite. To simplify the mathematical representation, we use the contact angle φ to denote the relative location between a LoRa ED and its serving satellite, i.e., the Earth-centered zenith angle, and the maximum contact angle φ_m is given as [8]

$$\varphi_m = \cos^{-1} \left(\frac{R}{R + H} \right). \quad (2)$$

According to the characteristics of the BPP constellation model, the PDF of the contact angle is given by [8]

$$f_\varphi(x) = \frac{N_s}{2} \sin x \exp \left[-\frac{N_s}{2} (1 - \cos x) \right], \quad x \geq 0. \quad (3)$$

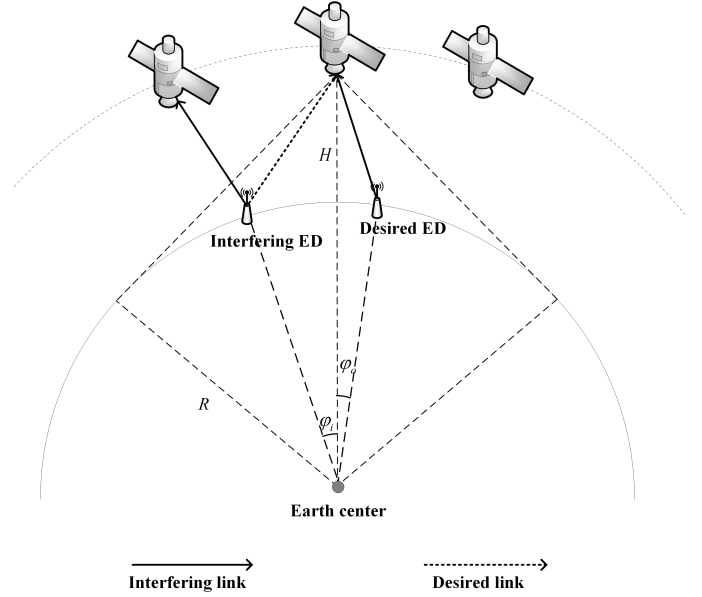


Fig. 1. An illustration of the network model for LoRa-based LEO satellite constellations.

Moreover, given the contact angle φ , the distance between a LoRa ED and a LEO satellite can be obtained using the basic cosine theorem as [9]

$$d(\varphi) = \sqrt{(R + H)^2 + R^2 - 2R(R + H) \cos \varphi}. \quad (4)$$

B. Channel Model

1) *Large-scale fading*: For the sake of simplicity, the free space path-loss model is adopted to characterize the large-scale fading, which is suitable for Internet of remote things where the LoRa EDs are typically deployed in open remote areas.¹ Specifically, it is given as

$$L(d(\varphi)) = \left(\frac{c}{4\pi f_c d(\varphi)} \right)^2, \quad (5)$$

where c is the speed of light and f_c is the carrier frequency.

2) *Small-scale fading*: In addition, the small-scale fading of the desired and interfering LoRa EDs of class k , i.e., $h_{i,k}$ and $h_{d,k}$, follows an independent and identically distributed (i.i.d.) shadowed Rician (SR) fading with Nakagami fading coefficient m , the half average power of scattered component b_0 and the average power of the line-of-sight component Ω . The SR channel gain $|h|^2$ can be approximated by a Gamma random variable with its CDF and PDF denoted as [9]

$$F_{|h|^2}(x) \approx \frac{1}{\Gamma(\alpha)} \gamma \left(\alpha, \frac{x}{\beta} \right), \quad x \geq 0, \quad (6)$$

$$f_{|h|^2}(x) \approx \frac{1}{\beta^\alpha \Gamma(\alpha)} x^{\alpha-1} \exp \left(-\frac{x}{\beta} \right), \quad x \geq 0, \quad (7)$$

where $\Gamma(\cdot)$ denotes the Gamma function, $\gamma(\cdot, \cdot)$ is the lower incomplete Gamma function, $\alpha \triangleq \frac{m(2b_0 + \Omega)^2}{4mb_0^2 + 4mb_0\Omega + \Omega^2}$ and

¹It is worth noting that the additional path-loss caused by atmospheric absorption and natural/artificial obstacles can be easily incorporated into our channel model by adding the corresponding path-loss factor into the large-scale fading.

$\beta \triangleq \frac{4mb_0^2 + 4mb_0\Omega + \Omega^2}{m(2b_0 + \Omega)}$ are the shape and scale parameters, respectively.

C. Signal Model

As depicted in Fig. 1, we consider the aggregated inter-ED interference at one of the serving satellites that comes from all the active LoRa EDs other than the desired ED within its coverage region. For our considered LoRa-based LEO satellite constellations, inter-ED interference consists of the same SF (co-SF) interference and the different SF (inter-SF) interference. Given the waveform properties of CSS modulation, different SFs are quasi-orthogonal and thus inter-SF interference from different classes of LoRa EDs can be negligible [7]. Moreover, we denote $\kappa \in [0, 1]$ as the interference mitigation factor, which captures the impact of random access on the overall system performance.

Accordingly, let us denote $s_{o,k}$ and $s_{i,k}$ as the unit power transmitted signal from the desired and interfering LoRa EDs of class k , respectively, while the received signal of class k can be expressed as

$$r_k = \underbrace{\sqrt{P_t GL(d(\varphi_{o,k}))} h_{o,k} s_{o,k}}_{\text{desired signal}} + \underbrace{w_k}_{\text{noise}} + \underbrace{\kappa \sum_{i \in \Phi_k^A \setminus o} \sqrt{P_t GL(d(\varphi_{i,k}))} h_{i,k} s_{i,k}}_{\text{interfering signal}}, \quad (8)$$

where G represents the satellite antenna gain, $w_k \sim \mathcal{CN}(0, \sigma^2)$ denotes the complex circularly symmetric additive white Gaussian noise (AWGN). Note that $\sigma^2 = -174 + N_F + 10 \log_{10} B$, with N_F representing the receiver's noise figure.

III. PERFORMANCE ANALYSIS

To evaluate the system-level performance, we define the uplink coverage probability and area spectral efficiency as the performance metrics, which characterize the scalability and capacity of LoRa-based LEO satellite constellations, respectively. In the following, we first analyze the conditional access probability and both the system-level performance metrics are obtained subsequently.

A. Conditional Access Probability Analysis

For a typical LoRa network, the successful transmission occurs only if both the signal-to-noise ratio (SNR) and the signal-to-interference ratio (SIR) of the received signal exceed their demodulation thresholds, and thereby the conditional access probability P_s , for a given contact angle $\varphi_{o,k}$, is defined as [10]

$$P_{s|\varphi_{o,k}} = P_{SNR|\varphi_{o,k}} P_{SIR|\varphi_{o,k}}, \quad (9)$$

where $P_{SNR|\varphi_{o,k}}$ and $P_{SIR|\varphi_{o,k}}$ denote the connection probability and the capture probability for a given contact angle $\varphi_{o,k}$, respectively. In particular, the connection probability $P_{SNR|\varphi_{o,k}}$ is defined as the probability that the SNR of the

received signal exceeds the demodulation threshold, which can be derived as

$$\begin{aligned} P_{SNR|\varphi_{o,k}} &= \Pr \left\{ \frac{P_t GL(d(\varphi_{o,k})) |h_{o,k}|^2}{\sigma^2} \geq \gamma_k \right\} \\ &= 1 - F_{|h_{o,k}|^2} \left(\frac{\sigma^2 \gamma_k}{P_t GL(d(\varphi_{o,k}))} \right) \\ &\stackrel{(a)}{\approx} 1 - \frac{1}{\Gamma(\alpha)} \gamma \left(\alpha, \frac{\sigma^2 \gamma_k}{\beta P_t GL(d(\varphi_{o,k}))} \right), \end{aligned} \quad (10)$$

where γ_k is the SF-specific SNR demodulation threshold of class k and step (a) follows from the substitution of the CDF given in (6). Additionally, the capture probability $P_{SIR|\varphi_{o,k}}$ is defined as the probability that the SIR of the received signal exceeds the corresponding demodulation threshold, which can be expressed as

$$P_{SIR|\varphi_{o,k}} = \Pr \left\{ \frac{P_t GL(d(\varphi_{o,k})) |h_{o,k}|^2}{\kappa \sum_{i \in \Phi_k^A \setminus o} P_t GL(d(\varphi_{i,k})) |h_{i,k}|^2} \geq \gamma_I \right\}, \quad (11)$$

where γ_I is the SIR demodulation threshold.

Herein, we denote $I_k = \kappa \sum_{i \in \Phi_k^A \setminus o} P_t GL(d(\varphi_{i,k})) |h_{i,k}|^2$ as the aggregated inter-ED interference. For an accurate performance analysis, we need to investigate the statistical distribution of I_k . However, due to the randomness of both channel fading and spatial point process, it is challenging to obtain the accurate statistical distribution of I_k . To tackle this challenge, we approximate the impact of the aggregated inter-ED interference by that of the average inter-ED interference, i.e., $I_k \approx \mathbb{E}[I_k] = \bar{I}_k$ [5]. As a result, the capture probability P_{SIR} can be approximated as

$$P_{SIR|\varphi_{o,k}} \approx \Pr \left\{ \frac{P_t GL(d(\varphi_{o,k})) |h_{o,k}|^2}{\bar{I}_k} \geq \gamma_I \right\}, \quad (12)$$

with

$$\begin{aligned} \bar{I}_k &= \mathbb{E}_{I_k} \left[\kappa \sum_{i \in \Phi_k^A \setminus o} P_t GL(d(\varphi_{i,k})) |h_{i,k}|^2 \right] \\ &\stackrel{(b)}{=} 2\pi R^2 \kappa p_k \lambda_k P_t G \int_0^{\varphi_m} L(d(\varphi)) \mathbb{E}_{|h|^2} [|h|^2] \sin \varphi d\varphi \\ &\stackrel{(c)}{\approx} 2\pi R^2 \kappa p_k \rho_k \lambda P_t G \alpha \beta \underbrace{\int_0^{\varphi_m} L(d(\varphi)) \sin \varphi d\varphi}_{\mathcal{I}}, \end{aligned} \quad (13)$$

where step (b) follows from the Campbell's theorem [11] and the fact that the i.i.d. channel fading is independent from the spatial point process, while step (c) follows from the mean value of the approximated Gamma distribution of channel fading. Moreover, the integral \mathcal{I} can be calculated as

$$\begin{aligned} \mathcal{I} &= \int_0^{\varphi_m} \frac{c_0^2 \sin \varphi}{(R+H)^2 + R^2 - 2R(R+H) \cos \varphi} d\varphi \\ &\stackrel{(d)}{=} \int_{\cos \varphi_m}^1 \frac{c_0^2}{(R+H)^2 + R^2 - 2R(R+H)u} du \\ &\stackrel{(e)}{=} \int_{v_1}^{v_2} \frac{c_0^2}{2R(R+H)v} dv \\ &= \frac{c_0^2}{2R(R+H)} \ln \left(\frac{v_2}{v_1} \right), \end{aligned} \quad (14)$$

where step (d) follows $u = \cos \varphi$, step (e) follows $v = (R+H)^2 + R^2 - 2R(R+H)u$ and we denote $v_1 = H^2$, $v_2 = (R+H)^2 + R^2 - 2R(R+H)\cos \varphi_m$, $c_0 = \frac{c}{4\pi f_c}$ for simplicity.

Hence, the approximate capture probability can be simplified as

$$\begin{aligned} P_{SIR|\varphi_{o,k}} &\approx \Pr \left\{ \frac{P_t GL(d(\varphi_{o,k})) |h_{o,k}|^2}{\bar{I}_k} \geq \gamma_I \right\} \\ &= 1 - F_{|h_{o,k}|^2} \left(\frac{\bar{I}_k \gamma_I}{P_t GL(d(\varphi_{o,k}))} \right) \\ &\stackrel{(f)}{\approx} 1 - \frac{1}{\Gamma(\alpha)} \gamma \left(\alpha, \frac{c_0^2 \pi R \kappa p_k \rho_k \lambda \alpha \gamma_I \ln \left(\frac{v_2}{v_1} \right)}{(R+H)L(d(\varphi_{o,k}))} \right), \end{aligned} \quad (15)$$

where step (f) leverages the approximated Gamma distribution of channel fading described in (6).

B. System-level Performance Analysis

The uplink coverage probability P_c is defined as the probability that the desired signal of a randomly chosen LoRa ED can be successfully demodulated, which characterizes the scalability of LoRa-based LEO satellite constellations. As such, P_c can be expressed as

$$P_c = \mathbb{E}_{\varphi_{o,k}} [P_{s|\varphi_{o,k}}], \quad (16)$$

where $P_{s|\varphi_{o,k}}$ denotes the conditional access probability for a given contact angle $\varphi_{o,k}$. Therefore, facilitated by the PDF of contact angle $\varphi_{o,k}$ given in (3), the uplink coverage probability can be formulated as

$$\begin{aligned} P_c &= \mathbb{E}_{\varphi_{o,k}} [P_{s|\varphi_{o,k}}] = \mathbb{E}_{\varphi_{o,k}} [P_{SNR|\varphi_{o,k}} P_{SIR|\varphi_{o,k}}] \\ &= \int_0^{\varphi_m} \frac{N_s}{2} \sin \varphi_{o,k} \exp \left[-\frac{N_s}{2} (1 - \cos \varphi_{o,k}) \right] \\ &\quad \times \left[1 - \frac{1}{\Gamma(\alpha)} \gamma \left(\alpha, \frac{c_0^2 \pi R \kappa p_k \rho_k \lambda \alpha \gamma_I \ln \left(\frac{v_2}{v_1} \right)}{(R+H)L(d(\varphi_{o,k}))} \right) \right] \\ &\quad \times \left[1 - \frac{1}{\Gamma(\alpha)} \gamma \left(\alpha, \frac{\sigma^2 \gamma_k}{\beta P_t GL(d(\varphi_{o,k}))} \right) \right] d\varphi_{o,k}. \end{aligned} \quad (17)$$

Corollary 1. *The uplink coverage probability P_c is a monotonically decreasing function of the EDs' density λ .*

Proof: Note that P_c for a given contact angle $\varphi_{o,k}$ can be expressed as $Z \times \left[1 - \frac{1}{\Gamma(\alpha)} \gamma \left(\alpha, \frac{c_0^2 \pi R \kappa p_k \rho_k \lambda \alpha \gamma_I \ln \left(\frac{v_2}{v_1} \right)}{(R+H)L(d(\varphi_{o,k}))} \right) \right]$, where

$$\begin{aligned} Z &= \frac{N_s}{2} \sin \varphi_{o,k} \exp \left[-\frac{N_s}{2} (1 - \cos \varphi_{o,k}) \right] \\ &\quad \times \left[1 - \frac{1}{\Gamma(\alpha)} \gamma \left(\alpha, \frac{\sigma^2 \gamma_k}{\beta P_t GL(d(\varphi_{o,k}))} \right) \right], \end{aligned} \quad (18)$$

is independent of the EDs' density λ . Since the lower incomplete gamma function $\gamma \left(\alpha, \frac{c_0^2 \pi R \kappa p_k \rho_k \lambda \alpha \gamma_I \ln \left(\frac{v_2}{v_1} \right)}{(R+H)L(d(\varphi_{o,k}))} \right)$ is increasing with respect to its second argument, P_c is a monotonically decreasing function of the EDs' density λ . The proof is completed. ■

Furthermore, the area spectral efficiency η_k measures the information rate per unit area (in bit/s/m²), which characterizes the network capacity of LoRa-based LEO satellite constellations and can be expressed as [7]

$$\eta_k = p_k \rho_k \lambda B \log_2 (1 + \gamma_k) P_c, \quad (19)$$

where P_c is given by (17).

Corollary 2. *The area spectral efficiency η_k is a unimodal function of the EDs' density λ .*

Proof: We first notice that $\alpha \triangleq \frac{m(2b_0+\Omega)^2}{4mb_0^2+4mb_0\Omega+\Omega^2} = \frac{4mb_0^2+4mb_0\Omega+m\Omega^2}{4mb_0^2+4mb_0\Omega+\Omega^2} > 1$ for $m > 1$. Hence, the lower incomplete gamma function $\gamma \left(\alpha, \frac{c_0^2 \pi R \kappa p_k \rho_k \lambda \alpha \gamma_I \ln \left(\frac{v_2}{v_1} \right)}{(R+H)L(d(\varphi_{o,k}))} \right)$ is convex with respect to its second argument in this case. Now, noting that the second argument of this lower incomplete gamma function is linearly increasing in λ , P_c , for a given contact angle $\varphi_{o,k}$, is a concave function decreasing with respect to λ according to Corollary 1. Therefore, since η_k is the product of P_c and a positive linear function of λ , i.e., $p_k \rho_k \lambda B \log_2 (1 + \gamma_k)$, the area spectral efficiency is a pseudoconcave or unimodal function of the EDs' density [12]. The proof is completed. ■

With this, we complete the performance analysis, which not only reveals novel engineering insights but also, with the help of Corollaries 1 and 2, demonstrates the existence of a unique maxima for the area spectral efficiency, thus motivating the need to optimally select the EDs' density.

IV. NUMERICAL RESULTS AND DISCUSSION

In this section, we validate our proposed analytical framework through Monte-Carlo simulations, which also provide some valuable insights into the practical design and implementation of LoRa-based LEO satellite constellations for IoT communications. The simulation setup is illustrated as follows. Without loss of generality, we set $N_s = 1000$, $R = 6371$ km, $H = 500$ km, $L = 50$ bytes, $T_p = 3600$ s, $f_c = 868$ MHz, $B = 125$ kHz, $P_t = 16$ dBm, $N_F = 6$ dB, $G = 22.6$ dBi, and $\kappa = 10^{-3}$. Moreover, we assume that $N_p = 8$, $C = 1$, $E = 0$, and $C_r = 1$ as in [7]. The SR fading parameters are set as $m = 5.21$, $b_0 = 0.251$, and $\Omega = 0.278$, which is in accordance with [9]. In addition, the SF-specific SNR demodulation threshold γ_k is $-6, -9, -12, -15, -17.5, -20$ dB for k from 7 to 12, respectively, and the SIR demodulation threshold γ_I is set to be 6 dB [10].

Figures 2(a) and 2(b) demonstrate the uplink coverage probability and area spectral efficiency of LoRa-based LEO satellite constellations versus the EDs' density, respectively. First, it can be observed that the numerical results of both performance metrics match well with their theoretical results, which substantiates our proposed analytical framework. The effectiveness of approximation in (12) is also validated, which shows that our performance analysis holds tight in practice. Second, as illustrated in Fig. 2(a), the uplink coverage probability P_c is a monotonically decreasing function of the EDs' density and it can be observed that higher coverage probability, i.e., better scalability performance, can be achieved

for smaller SFs because larger SFs could be more prone to the aggregated inter-ED interference due to the longer ToA of LoRa EDs given by (1). Third, different from the uplink coverage probability, the area spectral efficiency is a unimodal function of the EDs' density, as shown in Fig. 2(b), which corroborates our analysis once again, while the optimal value of λ under specific parameter settings can be obtained through some search methods.

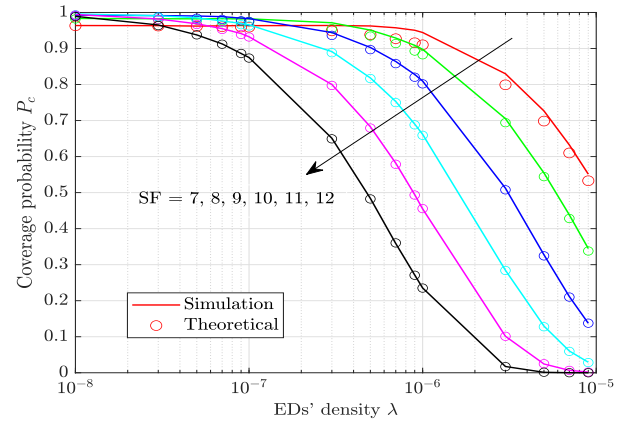
In addition, it can be seen that the maximum achievable area spectral efficiency increases dramatically for smaller SFs due to their better scalability performance. Furthermore, by inspecting Figures 2(a) and 2(b), it can be observed that higher coverage probability could be achieved for smaller EDs' density, i.e., $\lambda \leq 10^{-7}$, while higher area spectral efficiency could be obtained for relatively larger EDs' density, i.e., $\lambda \geq 10^{-6}$. Hence, by tuning the EDs' density, a trade-off occurs between the scalability and network capacity of LoRa-based LEO satellite constellations. Therefore, the performance optimization of our considered LoRa-based LEO satellite constellations by employing appropriate network deployment and efficient resource allocation schemes is worth investigating [13]. Moreover, extending our analytical framework to multi-tier LEO satellite constellations and/or space-air-ground integrated network [14] could also serve as an interesting topic for future research.

V. CONCLUSION

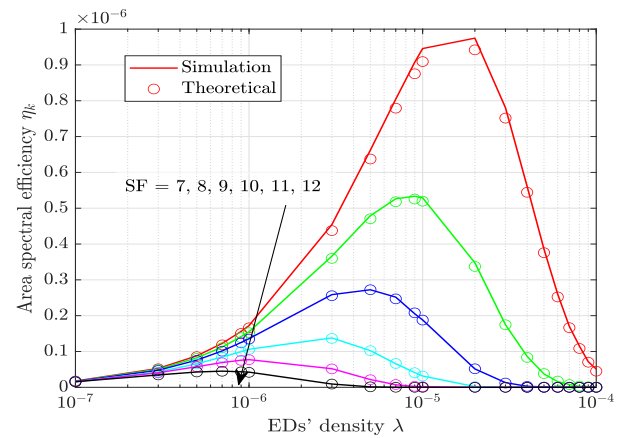
In this letter, a novel analytical framework for characterizing the system-level performance of LoRa-based LEO satellite constellations was formulated based on spherical SG. Both the channel characteristics of satellite communications for IoT applications and the unique features of LoRa networks were incorporated into the proposed system model to derive tractable analytical expressions for the uplink coverage probability and area spectral efficiency. Numerical simulations were conducted to verify the accuracy of our proposed analytical framework and also provide some insightful guidelines for the practical design and implementation of LoRa-based LEO satellite constellations for IoT communications. Overall, we believe that our work will set a solid foundation for further investigations of LoRa-based non-terrestrial networks (NTNs) in the future.

REFERENCES

- [1] J. P. Shanmuga Sundaram, W. Du, and Z. Zhao, "A survey on LoRa networking: Research problems, current solutions, and open issues," *IEEE Commun. Surveys Tuts.*, vol. 22, no. 1, pp. 371-388, 1st Quart., 2020.
- [2] N. Saeed, A. Elzanaty, H. Almorad, H. Dahrouj, T. Y. Al-Naffouri, and M. -S. Alouini, "CubeSat communications: Recent advances and future challenges," *IEEE Commun. Surveys Tuts.*, vol. 22, no. 3, pp. 1839-1862, 3rd Quart., 2020.
- [3] M. Centenaro, C. E. Costa, F. Granelli, C. Sacchi, and L. Vangelista, "A survey on technologies, standards and open challenges in satellite IoT," *IEEE Commun. Surveys Tuts.*, vol. 23, no. 3, pp. 1693-1720, 3rd Quart., 2021.
- [4] Q. Yu, D. Mishra, H. Wang, D. He, J. Yuan, and M. Matthaiou, "Closed-form access probability analysis of LoRa-based LEO satellite IoT," accepted for presentation at *IEEE ICC*, Jun. 2025.
- [5] C. C. Chan, B. Al Homssi, and A. Al-Hourani, "A stochastic geometry approach for analyzing uplink performance for IoT-over-satellite," in *Proc. IEEE ICC*, May 2022, pp. 1-6.



(a) Uplink coverage probability



(b) Area spectral efficiency

Fig. 2. System-level performance of LoRa-based LEO satellite constellations versus the EDs' density λ for (a) uplink coverage probability and (b) area spectral efficiency.

- [6] A. Talgat, M. A. Kishk, and M. -S. Alouini, "Stochastic geometry-based uplink performance analysis of IoT over LEO satellite communication," *IEEE Trans. Aerosp. Electron. Syst.*, vol. 60, no. 4, pp. 4198-4213, Aug. 2024.
- [7] L. -T. Tu, A. Bradai, Y. Pousset, and A. I. Aravanis, "On the spectral efficiency of LoRa networks: Performance analysis, trends and optimal points of operation," *IEEE Trans. Commun.*, vol. 70, no. 4, pp. 2788-2804, Apr. 2022.
- [8] A. Al-Hourani, "An analytic approach for modeling the coverage performance of dense satellite networks," *IEEE Wireless Commun. Lett.*, vol. 10, no. 4, pp. 897-901, Apr. 2021.
- [9] H. Jia, C. Jiang, L. Kuang, and J. Lu, "An analytic approach for modeling uplink performance of mega constellations," *IEEE Trans. Veh. Technol.*, vol. 72, no. 2, pp. 2258-2268, Feb. 2023.
- [10] O. Georgiou and U. Raza, "Low power wide area network analysis: Can LoRa scale?," *IEEE Wireless Commun. Lett.*, vol. 6, no. 2, pp. 162-165, Apr. 2017.
- [11] M. Haenggi, *Stochastic Geometry for Wireless Networks*. Cambridge, U.K.: Cambridge Univ. Press, 2012.
- [12] M. Avriel, W. E. Diewert, S. Schaible, and I. Zang, *Generalized Convexity*. Philadelphia, PA, USA: SIAM, 2010.
- [13] Y. Qin, M. A. Kishk, and M. -S. Alouini, "Coverage analysis and trajectory optimization for aerial users with dedicated cellular infrastructure," *IEEE Trans. Wireless Commun.*, vol. 23, no. 4, pp. 3042-3056, Apr. 2024.
- [14] Y. Liu *et al.*, "Space-air-ground integrated networks: Spherical stochastic geometry-based uplink connectivity analysis," *IEEE J. Sel. Areas Commun.*, vol. 42, no. 5, pp. 1387-1402, May 2024.